Structural and functional properties of V156K and A158E mutants of apolipoprotein A-I in the lipid-free and lipid-bound states

Jong-Min Han,* Tae-Sook Jeong,* Woo Song Lee,* Inho Choi,† and Kyung-Hyun Cho*,1,2

National Research Laboratory of Lipid Metabolism and Atherosclerosis,* Korea Research Institute of Bioscience and Biotechnology, Yuseong-gu, 305-333, South Korea; School of Biotechnology and School of Biological Resources,† Yeungnam University, Kyungsan, 712-749, South Korea

Abstract **Val156 of apolipoprotein A-I (apoA-I) was found to be a key amino acid in the structure and function of high density lipoprotein (HDL) (*J. Biol. Chem.*, 275: 26821–26827, 2000). To determine more precisely the functions of the individual amino acids proximal to Val156, serial point mutants of proapoA-I, including V156K, D157K, and A158E, were overexpressed and purified to at least 95% purity. In the lipid-free state, A158E exhibited the most profound self-associative patterns and the least pronounced dimyristoyl phosphatidylcholine (DMPC) clearance activities. In the lipid-bound state, A158E formed a larger reconstituted HDL (rHDL) with palmitoyloleoyl phosphatidylcholine (POPC), ~120 Å, whereas other mutants and the wild type (WT) formed 97 Å of POPC-rHDL. Cross-linking analysis revealed that A158E-rHDL harbored at least four protein molecules in the particle, while other rHDL conformations contained only two protein molecules. All of the POPC-rHDL produced smaller HDL, around 78 Å, after 24 h of incubation in the presence of low density lipoprotein at 37°C. V156K and A158E exhibited decreased lecithin:cholesterol acyltransferase activation activity in the POPC-rHDL state, showing <2% of WT reactivity (apparent V_{max}/K_m). A158E also displayed markedly different properties in secondary structure, and its accessibility to proteolytic enzymes is different. These results suggest that the two amino acids in helix 6, Val156 and Ala158, are critical to both the structure and function of rHDL.**—Han, J-M., T-S. Jeong, W. S. Lee, I. Choi, and K-H. Cho. **Structural and functional properties of V156K and A158E mutants of apolipoprotein A-I in the lipid-free and lipid-bound state. *J. Lipid Res.* 2005.** 46: **589–596.**

Supplementary key words apoA-I mutants • reconstituted HDL • lecithin:cholesterol acyltransferase • structure-function • middle mobile region

Apolipoprotein A-I (apoA-I) constitutes the major protein component of HDL (1, 2). It is responsible for the major functions of HDL lipid binding and solubilization, cholesterol removal from peripheral cells, and lecithin: cholesterol acyltransferase (LCAT) activation. Numerous reports have demonstrated that many of the functions of HDL are highly dependent on the conformation of apoA-I, most notably, the rearrangement of HDL in reverse cholesterol transport (3, 4) and its interaction with the HDL receptor, scavenger receptor class B type I, on the cell surfaces (5, 6). Therefore, a great deal of effort has been focused on the delineation of the structural and functional regions of apoA-I. The central region of apoA-I, spanning residues 143–165, has been implicated in the activation of LCAT and the regulation of high density lipoprotein (HDL) structural rearrangement.

Recombinant human proapoA-I has previously been reported to exhibit the same general properties and functions as plasma apoA-I, in both lipid-free and lipid-bound states (7). Previously, Cho and Jonas (8) reported that Valine156 was a key amino acid with regard to the structure and functions of apoA-I, because the recombinant V156E mutant behaved differently from the wild type (WT) in both the lipid-free and lipid-bound states. In the lipid-free state, the V156E mutant exhibited greater protein stability and was quite resistant to self-association, as compared with WT apoA-I. Furthermore, in the palmitoyloleoyl phosphatidylcholine reconstituted HDL (POPC-rHDL) state, the V156E did not rearrange its particles to produce smaller particles in the presence of low density lipoprotein (LDL), and exhibited minimal reactivity to LCAT activation. These results indicated that a few of the

Abbreviations: ApoA-I, apolipoprotein A-I; BS_3, bis-sulfosuccinimidyl suberate; DMPC, dimyristoyl phosphatidylcholine; HDL, high density lipoprotein; LCAT, lecithin:cholesterol acyltransferase; LDL, low density lipoprotein; LPDS, lipoprotein-deficient serum; POPC, palmitoyloleoyl phosphatidylcholine; rHDL, reconstituted HDL; WMF, wavelength of maximum fluorescence; WT, wild type.

[1] To whom correspondence should be addressed.
e-mail: chok@kribb.re.kr

[2] Present address of K-H. Cho: School of Biotechnology Yeungnam University, Kyungsan, 712-749, South Korea.

Manuscript received 23 November 2004.

Published, JLR Papers in Press, February 16, 2005.
DOI 10.1194/jlr.M400468-JLR200

important aspects of apoA-I are highly dependent on the Val156 residue. Another naturally occurring mutant, A158E, was also reported as a natural mutant, apoA-I Münster-2(B), although its biochemical and biophysical characteristics have yet to be elucidated (9, 10). To determine more precisely the role of the amino acids adjacent to Val156, the amino acids Asp157 and Ala158 were mutated. Ala158, in particular, is located opposite Val156, as determined by a helical wheel analysis of helix 6 (143–164). This relationship is illustrated in **Fig. 1**.

The point mutant proteins were characterized in both the lipid-free and lipid-bound states after removal of the His-tag, with special attention paid to the hinge domain movement of apoA-I and LCAT activation.

MATERIALS AND METHODS

Radiolabeled [4-^{14}C]cholesterol was obtained from Amersham Biosciences (Seoul, Korea). L-α-phosphatidylcholine from egg yolk (egg PC), 1-palmitoyl-2-oleoylphosphatidylcholine, dimyristoyl phosphatidylcholine (DMPC), sodium cholate, and bis-sulfosuccinimidyl suberate (BS^3) were purchased from Sigma Chemical (St. Louis, MO). The quick-change site-directed mutagenesis kit was purchased from Stratagene (La Jolla, CA). The restriction enzymes were obtained from New England BioLabs (Beverly, MA). Enterokinase and the pET30a(+) expression vector, as well as *Escherichia coli* BL21 (DE3), were purchased from Roche (Germany) and Novagen (Madison, WI), respectively.

Vector construction, protein expression, and purification

The mutant cDNAs were generated by polymerase chain reaction based on the site-directed mutagenesis kit (Stratagene) using appropriately designed primers, as previously reported (8). Sequence of the primers' sense strand for point mutagenesis is as follows (mismatch codons are underlined): V156K, 5′-GACCGCGCCCGGGCCCATAAGGACGCGCTCCGGACG-3′; D157K, 5′-CGCGCGCGCACACGTGAAGGCGCTCCGGACGCAT-3′; A158E, 5′-GCGCGCGCACACGTGGACGAACTCCGGACGCACCTG-3′. The mutant constructs were verified by DNA sequencing and were subcloned into pET30a(+) expression vectors. The His-tagged WT proapoA-I and mutants were expressed and purified as previously reported (8, 11). To remove the His-tag (5 kDa) at the N-terminus of each protein, the proteins received enterokinase (Roche) digestion after synthesis of egg PC-rHDL with a molar ratio of 100:1 (egg PC-protein). The cleaved His-tag was removed by further delipidation and secondary Ni^{2+}-nitrilotriacetic acid column chromatography.

Synthesis of rHDL

Discoidal rHDL was prepared by the sodium cholate dialysis method (12) using initial molar ratios of POPC-cholesterol-apoA-I-sodium cholate of 95:5:1:150 (v/v/v/v). The rHDL particles for LCAT reaction were prepared by the same procedure, with the addition of a trace amount of [^{14}C]cholesterol. The rHDL particles were used without further purification, because they showed high homogeneity, and their sizes were determined from 8–25% native polyacrylamide gradient gel electrophoresis (Pharmacia Phast system) by comparison with standard globular proteins (AmershamPharmacia). The number of apoA-I molecules per rHDL particle, as well as the self-association properties of lipid-free proteins, were determined by cross-linking with BS_3 as described by Staros (13) and then analyzing the products of the reaction by SDS-PAGE on precast 8–25% gradient gels (AmershamPharmacia).

DMPC clearance assay

Interactions of the mutant proteins with DMPC were monitored by the method described by Pownall et al. (14), with slight modification. The mass ratio of DMPC to protein was 2:1 (w/w)

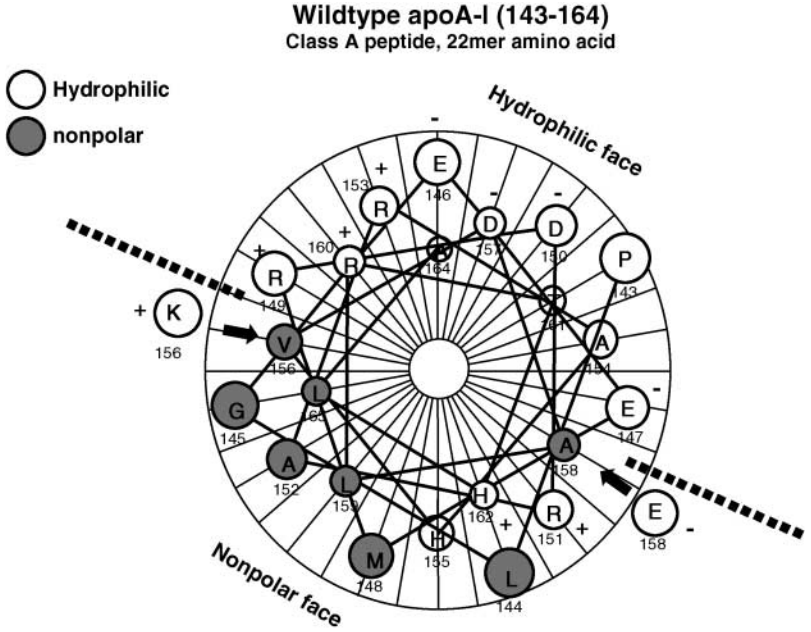

Fig. 1. Helical wheel representation of helix 6 (143–165 residues) in apolipoprotein A-I (apoA-I). Val156 and Ala158 are located at nearly opposite edges of the amphiphatic face. Note that the substitution of a charged amino acid (V156K or A158E) decreases the hydrophobicity in the amphiphatic boundary, as indicated by the dotted line. The wheel model was analyzed using Protean 5.07 software (DNASTAR) with a residue angle of 100.0 degrees at a pitch of 1.5.

in 0.76 ml of total reaction volume. The measurements were initiated after addition of DMPC and monitored at 325 nm every 2 min using an Agilent 8453 UV-visible spectrophotometer (Agilent Technologies, Waldbronn, Germany) equipped with a thermocontrolled cuvette holder adjusted to 24.5°C.

HDL particle rearrangement assay

To examine the conformational adaptability of the WT and mutant proteins in POPC-rHDL particles, changes of particle size were observed upon incubation with LDL, as well as the loss of phospholipid (15). To observe changes in the particle sizes, 100 μg of (protein) POPC-rHDL (0.1 ml) were incubated with 120 μg (protein) of human LDL (0.1 ml) at 37°C for the designated time interval up to 24 h. After incubation, aliquots of the samples were collected and stored at 4°C. The products were separated on 8–25% native polyacrylamide gradient gels, using the Pharmacia Phast System.

LCAT assay

The LCAT assay was carried out as described in detail previously (16), using the apoA-I and mutants in POPC-rHDL and human lipoprotein-deficient serum (LPDS, d < 1.21, bottom fraction) as a substrate and an enzyme source, respectively. The reaction mixture contained the radiolabeled cholesterol (1 μCi of [^{14}C]cholesterol/69 μg cholesterol/1 mg of apoA-I) in the POPC-rHDL with 4% defatted BSA and 4 mM β-mercaptoethanol. The reaction was initiated by the addition of 25 μl of the LPDS (5.4 mg/ml) and the mixture was incubated for 1 h at 37°C. The POPC-rHDLs were present in various concentrations, ranging from 1.0×10^{-6} to 2.5×10^{-7} M of apolipoprotein. The reaction was performed in duplicate, and background values were determined by omitting only the LPDS from the reaction tubes at each substrate concentration. Initial reaction velocities at each substrate concentration were determined by TLC analysis of the cholesterol and cholesterol esters, and Lineweaver-Burk plots were used to obtain the apparent K_m and V_{max} values by linear regression.

Protein sequencing

Protein samples for sequencing were electrotransferred onto a polyvinylidene difluoride membrane [Immobilon-P, (Millipore, Bedford, MA)] according to the protocol outlined by Matsudaira (17). The NH_2-terminal amino acid sequence of the excised band was determined with an Applied Biosystems Model 491A sequencer (Foster City, CA) located in the Korea Basic Research Institute (Daejeon, Korea).

Circular dichroism and fluorospectroscopy

The average α-helix content of proteins in the lipid-free and lipid-bound states were measured by circular dichroism spectroscopy, using a J-700 Spectropolarimeter (Jasco; Tokyo, Japan) located in the Korea Research Institute of Bioscience and Biotechnology (Daejeon, Korea). The spectra were obtained from 250 to 190 nm at 25°C in a 0.1 cm path-length quartz cuvette, using a 1.0 nm bandwidth, a speed of 50 nm/min, and a 4 s response time. The lipid-free proteins were diluted to 0.07 mg/ml to avoid self-association of the apolipoproteins (18), while lipid-bound proteins were diluted to 0.1 mg/ml. Four scans were accumulated and averaged. The α-helical content was calculated from the molar ellipticity at 222 nm (19). The wavelengths of maximum fluorescence (WMFs) of tryptophan residues in WT and mutants were determined from uncorrected spectra obtained on an LS50B spectrofluorometer (Perkin-Elmer, Norwalk, CT) using WinLab 4.00 (Perkin-Elmer) and a 1 cm path-length suprasil quartz cuvette (Fisher Scientific, Pittsburgh, PA). The samples were excited at 295 nm to avoid tyrosine fluorescence, and the emission spectra were scanned from 305 to 400 nm at room temperature.

Miscellaneous

LDL (1.019 < d < 1.063) was purified by ultracentrifugation [Beckman L8-M, Beckman, Palo Alto, CA)] using a 70.1 Ti rotor from human plasma after density adjustment with the addition of potassium bromide. After centrifugation, the LDL was extensively dialyzed against 10 mM Tris-HCl/5 mM EDTA/140 mM NaCl, pH 7.4, for 24 h to remove the KBr. Protein concentration was determined according to the Lowry protein assay as modified by Markwell et al. (20) or by using Bradford assay reagent (BioRad, Seoul, Korea) with BSA as a standard. Analysis of phosphorus (21) and free cholesterol (22) content was carried out according to the standard procedure.

RESULTS

Purification of apolipoproteins and BS_3 cross-linking

As His-tag-bound fusion proteins, both the WT and mutant proteins exhibited similar yields of expression in 30–40 mg of protein from 1 L of Luria-Bertani (LB) culture, except that ~15 mg of A158E was produced from the same culture. After His-tag removal, the proteins (29 kDa) were purified as shown in **Fig. 2A**, with densitometric scans confirming a purity of at least 95%. As shown in Fig. 2B, each protein exhibited significant self-associative properties in the lipid-free state, as determined by BS_3 cross-linking reaction at a protein concentration of 1 mg/ml. The cross-linked products displayed bands on the 8–25% gradient gel, indicating monomers, dimers, trimers, and tetramers. This result is consistent with a previous report that demonstrated the failure of the V156E mutant to self-associate (8). However, the replacement of Lys at the Val156 position resulted in the recovery of this ability, suggesting that the positively charged ε-amino group of Lys was able to participate in the cross-linking reaction. Interestingly, the A158E mutant exhibited the most obvious dimeric band formation (Fig. 2B), with a much weaker monomeric band among the proteins. This suggests that A158E preferentially forms multimers.

Apolipoprotein DMPC clearance

To characterize the phospholipids binding affinity of the recombinant WT and mutants, their ability to lyse DMPC liposomes was examined at 24.5°C. All proteins readily solubilized to DMPC liposomes (**Fig. 3**), and A158E exhibited remarkably slow clearance. In three independent assays under identical initial protein concentrations (0.15 mg/ml), half-lives ($T_{1/2}$) with regard to liposome clearance were as follows: 8 ± 1 min for WT, 6 ± 1 min for V156K, and 15 ± 2 min for A158E. In contrast to the enhanced clearance ability of V156E from the previous report (three times as fast as WT) (11), replacement of the positively charged amino acid (Lys) in the Val156 position resulted in a reduction in DMPC clearance activity.

Characterization of the POPC-rHDL

In the rHDL preparations, using a molar ratio of 95:5:1 (POPC-cholesterol-apoA-I) with each apolipoprotein resulted

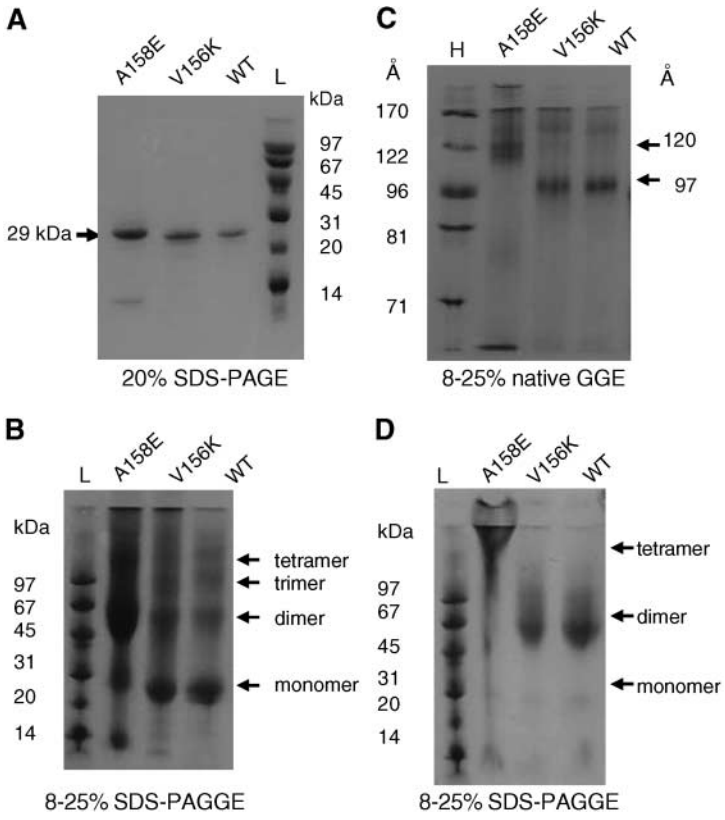

Fig. 2. Electrophoretic patterns of purified apolipoproteins. Lane L, molecular weight standard [low molecular weight (LMW) of AmershamPharmacia]; Lane H, the size marker [high molecular weight (HMW) standard of Amersham Pharmacia]. A, B: The purity of the proteins and self-associated products by bis-sulfosuccinimidyl suberate (BS_3) cross-linking, respectively, in the lipid-free state. The cross-linking reaction was carried out in 20 mM phosphate buffer, pH 7.4, with 1.0 mg/ml of each protein. C: Electrophoretic patterns of wild type (WT) and mutants in palmitoyloleoyl phosphatidylcholine-reconstituted HDL (POPC-rHDL) (8–25% native gel). D: The BS_3-cross-linked POPC-rHDL as visualized by 8–25% SDS-polyacrylamide gradient gel electrophoresis. All protein bands were visualized by Coomassie Blue staining.

in a major band of 96–97 Å POPC-rHDL size, as in the previous report (23), with the exception of A158E, which produced a much larger rHDL (>120 Å rHDL), as shown in Fig. 2C. BS_3 cross-linking with the rHDLs revealed that both WT and V156K-rHDL contained two apoA-I molecules per particle, whereas A158E-rHDL clearly contained multimeric proteins, because most of the bands appearing on the stacking gel were aggregated bands (Fig. 2D). These results indicate that A158E-rHDL, with at least four protein molecules, was bigger than both WT- and V156K-rHDL, and also exhibited highly increased cross-linking reactivity. The composition and sizes of the rHDLs are summarized in **Table 1**.

Particle size rearrangements

It has been established that WT apoA-I POPC-rHDLs (97 Å) undergo particle rearrangement to produce smaller

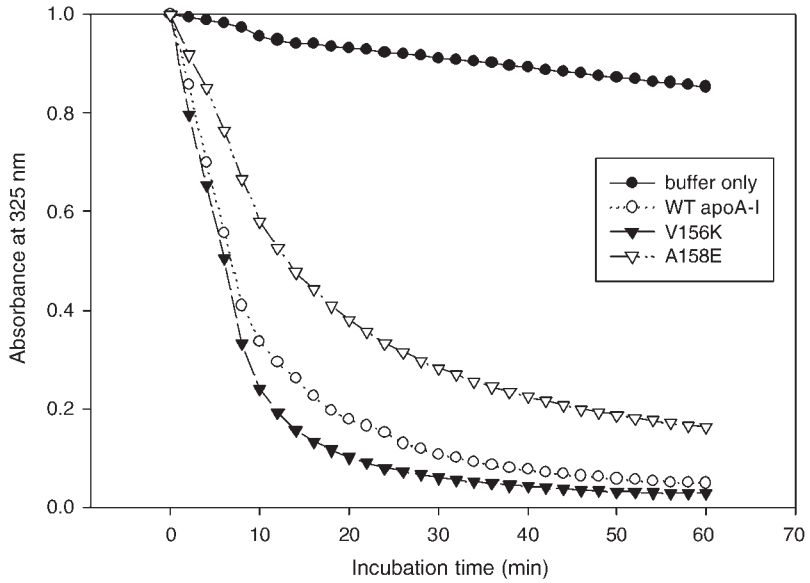

Fig. 3. Kinetics of the interaction of WT apoA-I and the other point mutants with dimyristoyl phosphatidylcholine multilamellar liposomes. Absorbance at 325 nm was monitored at 24.5°C at 2 min intervals.

TABLE 1. Compositional properties and spectroscopic data of apoA-I in lipid-free and rHDL state

	Molar Composition[a]					
	Initial	Final	α-Helicity	WMF	Size from GGE[b]	Number of Proteins/Particle
			%	*nm*	*Å*	
WT-POPC-rHDL	95:5:1	100 ± 8:5:1	74 ± 2 (52 ± 2)[c]	335 (337)	97	2
V156K-POPC-rHDL	95:5:1	103 ± 10:5:1	65 ± 2 (49 ± 3)	337 (338)	97	2
A158E-POPC-rHDL	95:5:1	152 ± 21:5:1	64 ± 3 (41 ± 2)	337 (344)	120	4

ApoA-I, apolipoprotein A-I; GGE, gradient gel electrophoresis; POPC, palmitoyloleoyl phosphatidylcholine; rHDL, reconstituted HDL; WMF, wavelength maximum fluorescence.

[a] The rHDLs were prepared by the sodium cholate dialysis method (12) and determined by the Markwell/Lowry protein assay (20) and analysis of phosphorus (21) and free cholesterol (22) on two independent reconstitution experiments.

[b] Determined from nondenaturating gradient gel (8–25%) electrophoresis using reference globular proteins (Fig. 2C).

[c] The number in parentheses indicates the proteins in the lipid-free state.

rHDLs (78 Å) after overnight incubation in the presence of LDL at 37°C. This rearrangement appears to occur via spontaneous phospholipid transfers and movement of the putative hinge domain of apoA-I. As shown in **Fig. 4**, all rHDLs (lane 1 of each panel) were converted completely to smaller rHDLs (78 Å) after 24 h of incubation (lane 5), regardless of mutant proteins. Interestingly, in the previous report, V156E-POPC-rHDL (110 Å) exhibited strong resistance to this particle rearrangement, and the resulting initial particle size persisted even after an equivalent incubation (8). However, the replacement of Lys in the same position produced a strikingly different result, allowing movement of the putative hinge domain.

Although its initial size was larger (120 Å) than that of other mutants, A158E-POPC-rHDL exhibited the same pattern of particle rearrangement (97 Å). This indicates that Ala158 is not a critical amino acid with regard to the regulation of conformational adaptability and/or hinge domain movement. Another interesting point is that the band intensity of A158E-78 Å-rHDL at 24 h was more pronounced than that of the WT and V156K, and no lipid-free apoA-I bands were detected on the bottom of the gel (Fig. 4). This indicates that the release of lipid-free apoA-I moiety did not occur after particle rearrangement.

Spectroscopic analysis

The α-helicity of recombinant proteins in the lipid-free and lipid-bound states was obtained by measuring the far-UV circular dichroic (CD) spectra. As shown in **Fig. 5**, the CD spectra patterns of mutants (with the exception of A158E) were similar to those of the WT, exhibiting two pronounced minima, at 208 nm and 222 nm, and a maxima at ~195 nm, a typical pattern for α-helical proteins. A158E, however, exhibited a different minimal and maximal ellipticity, at 206 nm and 192 nm, respectively, in the lipid-free state. As shown in Table 1, A158E in the lipid-free state exhibited the lowest degree of α-helical content at 41 ± 2%, whereas the WT α-helical content was 52 ± 2%. In the lipid-bound state, WT α-helicity increased to ~74%, as reported previously (8, 11), whereas V156K and A158E α-helicity increased to ~65%.

As shown in Table 1, Trp fluorescence scanning revealed that A158E had more red-shifted WMFs around 344 nm, which suggests that the Trps of A158E are more exposed to a polar environment than those contained in the WT (WMF, 337 nm). In the POPC-rHDL state, all proteins displayed consistently blue-shifted WMFs, indicating that their Trps are shifted into a more nonpolar phase. This suggests that Trp108 of A158E was more exposed to

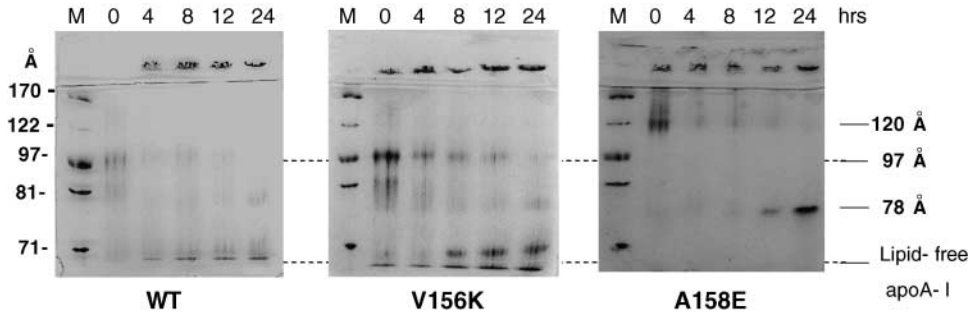

Fig. 4. Particle size rearrangement patterns of POPC-rHDL in the presence of low density lipoprotein (LDL) (8–25% native gradient gel electrophoresis). The reaction was initiated by adding 120 μg of human LDL (apo-B) to 100 μg of rHDL at 37°C. Aliquots of the incubation mixture were collected at designated time intervals and stored at 4°C until electrophoresis. Lane M, the HMW size marker, and incubation time is indicated in top of each lane. Protein bands were visualized by Coomassie Blue staining.

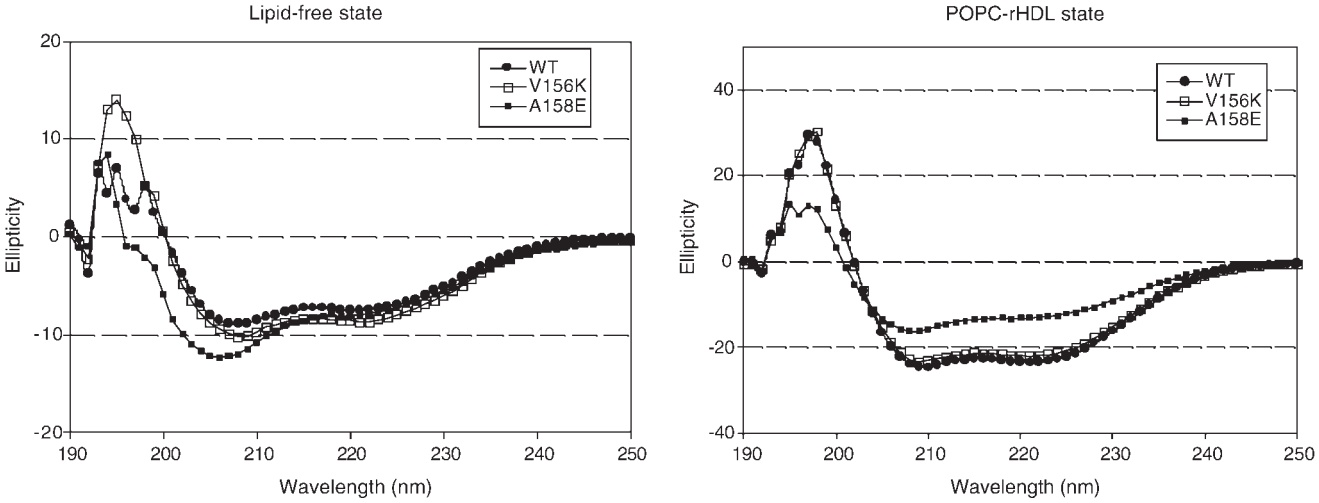

Fig. 5. Circular dichroism spectra of apolipoproteins in the lipid-free (0.07 mg/ml) and POPC-rHDL states (0.1 mg/ml). The spectra were recorded at 25°C, and four scans were accumulated and averaged.

a polar environment in both lipid-free and lipid-bound states, exhibiting WMFs at 344 nm and 337 nm, respectively. In V156K and A158E, more red-shifted Trp fluorescence values are consistent with their lower α-helicity in the lipid-bound state.

Activation of LCAT

ApoA-I is known to be a potent activator of LCAT, and its amino acids in the middle regions (residues 143–186) have been tentatively implicated in the activation. According to previous results, Val156 and Arg160 appear to be highly important in the activation of LCAT, because recombinant V156E and R160L in POPC-rHDL failed to activate LCAT, evidencing rHDL reactivity at <1% of WT levels (8, 11). As shown in **Fig. 6**, V156K-POPC-rHDL and A158E-POPC-rHDL served as poor substrates, with apparent V_{max} 0.3 ± 0.01 nmol and 0.5 ± 0.03 nmol cholesteryl ester/h, respectively. V156K-rHDL and A158E-rHDL exhibited almost completely abrogated reactivity, at <2% of WT levels, while D157K exhibited a reactivity of 20% of WT activity levels (**Table 2**). The apparent K_m and V_{max} values were determined from three independent experiments, with duplication by Lineweaver-Burk plot analysis (Table 2).

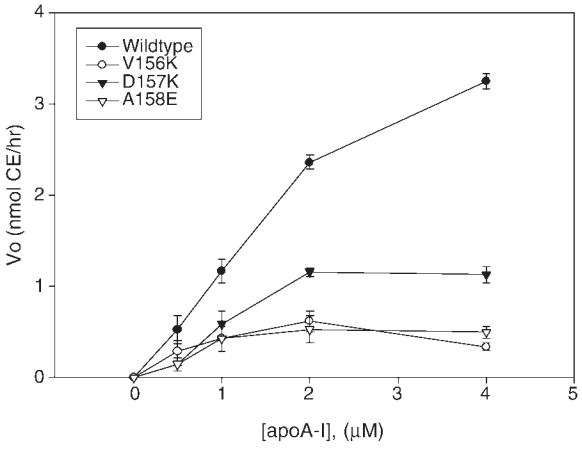

Fig. 6. Kinetics of lecithin:cholesterol acyltransferase reaction with POPC-rHDL substrates. The rHDLs were prepared at a molar ratio of 95:5:1:150 (POPC-free cholesterol-apoA-I-Na-cholate) with 4-[^{14}C]cholesterol. After the reaction, esterified products were isolated via TLC and quantitated via scintillation counting. Error bars indicate SD from triplicate experiments.

Mild chymotrypsin proteolysis

Limited proteolysis using chymotrypsin was employed to compare three-dimensional protein folding and protease accessibility in the WT and mutant proteins, in both the lipid-free and POPC-rHDL states. **Figure 7** shows the chymotryptic patterns of the various proteins, as visualized by SDS-PAGE. In the lipid-free and POPC-rHDL states, the main polypeptide product had a molecular weight of 25–26 kDa for WT and V156K, whereas A158E revealed a strikingly different proteolytic pattern with more susceptibility. Particularly in the lipid-free state, A158E and V156K proteolysis was completed within 10 or 40 min, respectively, because the major degraded fragments disappeared. In the POPC-rHDL state, the major fragments of both WT and V156K were visible until after 120 min of incubation, whereas A158E proteolysis was completed within 30 min.

TABLE 2. Reaction of rHDL particles with lecithin: cholesterol acyltransferase[a]

Apolipoproteins in rHDL	Apparent[b] V_{max}	Apparent K_m	Apparent V_{max}/ Apparent K_m
WT-POPC-rHDL	3.3 ± 0.3	0.9 ± 0.1	3.6 ± 0.2
V156K-POPC-rHDL	0.3 ± 0.01	6.2 ± 0.2	0.05 ± 0.01
D157K-POPC-rHDL	1.8 ± 0.1	2.4 ± 0.2	0.7 ± 0.2
A158E-POPC-rHDL	0.5 ± 0.03	6.0 ± 0.4	0.08 ± 0.03

[a] Values were expressed as the mean ± SD from three independent lecithin:cholesterol acyltransferase assays.

[b] The apparent kinetic parameters were determined by a linear regression analysis using a Lineweaver-Burk plot of the reciprocals of the reaction velocity versus the substrate concentrations.

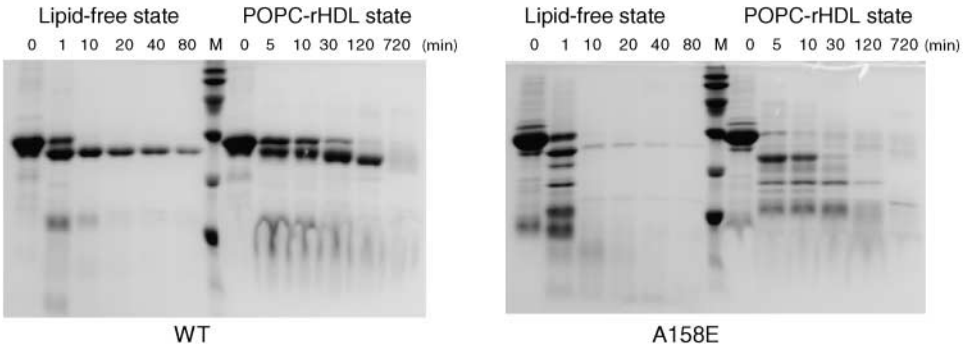

Fig. 7. Chymotrypsin digestion patterns for apolipoproteins in lipid-bound and lipid-free states. N-α-p-tosyl-L-lysine chloromethyl ketonehydrochloride (TLCK)-chymotrypsin was added at ratios of 1:100 and 1:200 (w/w) to the proteins in POPC-rHDL and in the lipid-free state, respectively. The reaction mixtures were incubated at 25°C, and aliquots were removed at the designated times, indicated at the top of the gel. The proteolytic products were separated by 16% SDS-PAGE, using the Tris-tricine buffer system, and protein bands were visualized by Coomassie Blue staining.

A158E's proteolytic susceptibility is consistent with the spectroscopic data from CD and fluorescence measurements, which revealed less α-helicity in the secondary structure, and more exposure of Trp to aqueous phase. Such peculiar structural properties might contribute to the high proteolytic sensitivity of A158E in both the lipid-free and lipid-bound states.

DISCUSSION

Numerous reports have described the natural and synthetic mutants of apoA-I, usually in attempts to delineate the structural and functional regions of apoA-I, or to understand changes in the physiological roles of HDL. In the current report, V156K and A158E manifested remarkably different properties in the lipid-free and lipid-bound states, especially within the context of their influence on the structure and function of rHDL. A helical wheel analysis of the helix 6 region (143–164) using Protean 5.07 (DNASTAR, Madison, WI) revealed that V156 and A158 are located on opposite edges, with an almost 180° interval angle of amphiphatic face, as illustrated in Fig. 1. Subsequently, substitution of charged amino acids for those at positions 156 and 158 resulted in increased hydrophilicity in the face of helix 6. Furthermore, the stability of helix 6 might be disturbed by the influence of the bulkier side chain of the substituted amino acid and the electrostatic repulsion occurring between the amino acids adjacent to V156K (between Arg149 and Lys156) and A158E (between Glu147 and Glu158). According to the computational calculations generated by the Protean 5.07 software, the proteins exhibited slightly different isoelectric points: 5.14, 5.23, and 5.07 for WT proapoA-I, V156K, and A158E, respectively. These proteins are expected to have charges of −10.03, −9.03, and −11.03 for WT, V156K, and A158E, respectively, at pH 7.0. These disturbances of the amphiphatic properties of helix 6 resulted in unexpected changes in various parameters, i.e., protein molecule numbers, particle size, and LCAT activation. For instance, V156K was markedly self-associative, and A158E exhibited the most profound formations of dimeric and trimeric bands via cross-linking (Fig. 1B). This indicates that the substitution of a negatively charged amino acid at position 158 resulted in more-profound monomers, monomer reactivity, and accessibility to BS_3. In addition, most of the protein bands of A158E appeared in the sample loading position in the POPC-rHDL state (Fig. 2D), indicating highly increased reactivity to BS_3 cross-linking, with a somewhat different conformation, and better accessibility to the cross-linker.

Numerous groups have attempted to identify the roles of the individual amino acid(s) essential in the activation of LCAT, with specific attention focused on the influence of apoA-I structure and conformation. Recent reports have identified the helix 6 domain, spanning amino acids 143–164 (24, 25), and the C-terminal domain as important to LCAT activation (26, 27). V156K-rHDL and A158E-rHDL particles served as poor substrates for LCAT activity, evidencing <2% of the activity of WT-rHDL. The substitution of the nonpolar amino acids, Val156 or Ala158, for charged amino acids on the hydrophobic face of helix 6 might lead to altered interactions between helix 6 of apoA-I and the 152–169 helix region of LCAT (28). Both of the mutations appear to have decreased face area hydrophobicity in the amphiphatic helix, as shown in Fig. 1, resulting from significant alterations to the hydrophobic face, as previously illustrated (29). With regard to the importance of the hydrophobic face, the positively charged amino acids of apoA-I are, presumably, instrumental to LCAT interaction, in that they are attracted to the negatively charged residues found in the LCAT helix, thereby facilitating the reaction (30). Taken together, this result and previous reports lead to the conclusion that the individual amino acid residues of Val156, Asp157, Ala158, Leu159, and Arg160 are all individually important with regard to LCAT activation.

The rHDL particle rearrangement assay, which was carried out to characterize the movement of the putative hinge domain, revealed that the amino acids adjacent to

Val156, as surmised in this study, are not critical to the movement of the hinge domain. A158E-rHDL also exhibited adequate rearrangement, despite its larger rHDL size (120 Å), within around four molecules of apoA-I. This result again was in agreement with previous reports that the locations of the LCAT activation domain and the hinge domain do not overlap, because R160L-rHDL was also defective with regard to LCAT activation but was unable to effect particle rearrangement (8). By combining several distinct characteristics of the mutants, we can surmise that the two mutants might play different physiological roles in circulation. Further study is clearly warranted to evaluate their abilities within the context of antiatherogenic potentials, such as antioxidant activity and cholesterol uptake and efflux activity. Regardless of support for the relevant model, i.e., the picket fence (31), belt model (32), and hairpin model (33) of apoA-I in the rHDL state, our data conclusively demonstrate that the two amino acids in helix 6 are critical to the function and structure of HDL.

This work was supported by Grant RO1-2002-000-00176-0 from the Basic Research Program of the Korea Science and Engineering Foundation. The authors express their gratitude to Dr W. S. Davidson, University of Cincinnati, for providing the wild-type proapoA-I expression vector (pET30-proapoAI).

REFERENCES

1. Frank, P. G., and Y. L. Marcel. 2000. Apolipoprotein A-I: structure-function relationships. *J. Lipid Res.* **41:** 853–872.
2. Brouillette, C. G., and G. M. Anantharamaiah. 1995. Structural models of human apolipoprotein A-I. *Biochim. Biophys. Acta.* **1256:** 103–129.
3. Cheung, M. C., J. P. Segrest, J. J. Albers, J. T. Cone, C. G. Brouillette, B. H. Chung, M. Kashyap, M. A. Glasscock, and G. M. Anantharamaiah. 1987. Characterization of high density lipoprotein subspecies: structural studies by single vertical spin ultracentrifugation and immunoaffinity chromatography. *J. Lipid Res.* **28:** 913–929.
4. Wald, J. H., E. S. Krul, and A. Jonas. 1990. Structure of apolipoprotein A-I in three homogeneous, reconstituted high density lipoprotein particles. *J. Biol. Chem.* **265:** 20037–20043.
5. Liu, T., M. Krieger, H. Y. Kan, and V. I. Zannis. 2002. The effects of mutations in helices 4 and 6 of apoA-I on scavenger receptor class B type I (SR-BI)-mediated cholesterol efflux suggest that formation of a productive complex between reconstituted high density lipoprotein and SR-BI is required for efficient lipid transport. *J. Biol. Chem.* **277:** 21576–21584.
6. Thuahnai, S. T., S. Lund-Katz, D. L. Williams, and M. C. Phillips. 2001. Scavenger receptor class B, type I-mediated uptake of various lipids into cells. Influence of the nature of the donor particle interaction with the receptor. *J. Biol. Chem.* **276:** 43801–43808.
7. McGuire, K. A., W. S. Davidson, and A. Jonas. 1996. High yield overexpression and characterization of human recombinant proapolipoprotein A-I. *J. Lipid Res.* **37:** 1519–1528.
8. Cho, K. H., and A. Jonas. 2000. A key point mutation (V156E) affects the structure and functions of human apolipoprotein A-I. *J. Biol. Chem.* **275:** 26821–26827.
9. Mahley, R. W., T. L. Innerarity, S. C. Rall, Jr., and K. H. Weisgraber. 1984. Plasma lipoproteins: apolipoprotein structure and function. *J. Lipid Res.* **25:** 1277–1294.
10. Menzel, H., R. Kladetzky, and G. Assmann. 1982. One-step screening method for the polymorphism of apolipoproteins A-I, A-II, and A-IV. *J. Lipid Res.* **23:** 915–922.
11. Cho, K. H., D. M. Durbin, and A. Jonas. 2001. Role of individual amino acids of apolipoprotein A-I in the activation of lecithin:cholesterol acyltransferase and in HDL rearrangements. *J. Lipid Res.* **42:** 379–389.
12. Matz, C. E., and A. Jonas. 1982. Micellar complexes of human apolipoprotein A-I with phosphatidylcholines and cholesterol prepared from cholate-lipid dispersions. *J. Biol. Chem.* **257:** 4535–4540.
13. Staros, J. V. 1982. N-hydroxysulfosuccinimide active esters: bis (N-hydroxysulfosuccinimide) esters of two dicarboxylic acids are hydrophilic, membrane-impermeant, protein cross-linkers. *Biochemistry.* **21:** 3950–3955.
14. Pownall, H. J., J. B. Massey, S. K. Kusserow, and A. M. Gotto, Jr. 1978. Kinetics of lipid-protein interactions: interaction of apolipoprotein A-I from human plasma high density lipoproteins with phosphatidylcholines. *Biochemistry.* **17:** 1183–1188.
15. Jonas, A., K. E. Kézdy, and J. H. Wald. 1989. Defined apolipoprotein A-I conformations in reconstituted high density lipoprotein discs. *J. Biol. Chem.* **264:** 4818–4824.
16. Minnich, A., X. Collet, A. Roghani, C. Cladaras, R. L. Hamilton, C. J. Fielding, and V. I. Zannis. 1992. Site-directed mutagenesis and structure-function analysis of the human apolipoprotein A-I. Relation between lecithin-cholesterol acyltransferase activation and lipid binding. *J. Biol. Chem.* **267:** 16553–16560.
17. Matsudaira, P. 1987. Sequence from picomole quantities of proteins electroblotted onto polyvinylidene difluoride membranes. *J. Biol. Chem.* **262:** 10035–10038.
18. Davidson, W. S., T. Hazlett, W. W. Mantulin, and A. Jonas. 1996. The role of apolipoprotein AI domains in lipid binding. *Proc. Natl. Acad. Sci. USA.* **93:** 13605–13610.
19. Chen, Y. H., J. T. Yang, and H. M. Martinez. 1972. Determination of the secondary structures of proteins by circular dichroism and optical rotatory dispersion. *Biochemistry.* **11:** 4120–4131.
20. Markwell, M. A., S. M. Haas, L. L. Bieber, and N. E. Tolbert. 1978. A modification of the Lowry procedure to simplify protein determination in membrane and lipoprotein samples. *Anal. Biochem.* **87:** 206–210.
21. Chen, P. S., T. Y. Toribara, and H. Warner. 1956. Microdetermination of phosphorus. *Anal. Chem.* **28:** 1756–1758.
22. Heider, J. G., and R. L. Boyett. 1978. The picomole determination of free and total cholesterol in cells in culture. *J. Lipid Res.* **19:** 514–518.
23. Jonas, A., J. H. Wald, K. L. Toohill, E. S. Krul, and K. E. Kézdy. 1990. Apolipoprotein A-I structure and lipid properties in homogeneous, reconstituted spherical and discoidal high density lipoproteins. *J. Biol. Chem.* **265:** 22123–22129.
24. Sorci-Thomas, M. G., L. Curtiss, J. S. Parks, M. J. Thomas, and M. W. Kearns. 1997. Alteration in apolipoprotein A-I 22-mer repeat order results in a decrease in lecithin:cholesterol acyltransferase reactivity. *J. Biol. Chem.* **272:** 7278–7284.
25. Holvoet, P., Z. Zhao, B. Vanloo, R. Vos, E. Deridder, A. Dhoest, J. Taveirne, E. Brouwers, E. Demarsin, Y. Engelborghs, M. Rosseneu, D. Collen, and R. Brasseur. 1995. Phospholipid binding and lecithin-cholesterol acyltransferase activation properties of apolipoprotein A-I mutants. *Biochemistry.* **34:** 13334–13342.
26. Sorci-Thomas, M. G., L. Curtiss, J. S. Parks, M. J. Thomas, M. W. Kearns, and M. Landrum. 1998. The hydrophobic face orientation of apolipoprotein A-I amphipathic helix domain 143–164 regulates lecithin:cholesterol acyltransferase activation. *J. Biol. Chem.* **273:** 11776–11782.
27. Ji, Y., and A. Jonas. 1995. Properties of an N-terminal proteolytic fragment of apolipoprotein AI in solution and in reconstituted high density lipoproteins. *J. Biol. Chem.* **270:** 11290–11297.
28. Fielding, C. J., and P. E. Fielding. 1995. Molecular physiology of reverse cholesterol transport. *J. Lipid Res.* **36:** 211–228.
29. Sorci-Thomas, M., M. W. Kearns, and J. P. Lee. 1993. Apolipoprotein A-I domains involved in lecithin-cholesterol acyltransferase activation. Structure:function relationships. *J. Biol. Chem.* **268:** 21403–21409.
30. Jonas, A. 1998. Regulation of lecithin cholesterol acyltransferase activity. *Prog. Lipid Res.* **37:** 209–234.
31. Phillips, J. C., W. Wriggers, Z. Li, A. Jonas, and K. Schulten. 1997. Predicting the structure of apolipoprotein A-I in reconstituted high-density lipoprotein disks. *Biophys. J.* **73:** 2337–2346.
32. Li, L., J. Chen, V. K. Mishra, J. A. Kurtz, D. Cao, A. E. Klon, S. C. Harvey, G. M. Anantharamaiah, and J. P. Segrest. 2004. Double belt structure of discoidal high density lipoproteins: molecular basis for size heterogeneity. *J. Mol. Biol.* **343:** 1293–1311.
33. Tricerri, M. A., A. K. Behling Agree, S. A. Sanchez, J. Bronski, and A. Jonas. 2001. Arrangement of apolipoprotein A-I in reconstituted high-density lipoprotein disks: an alternative model based on fluorescence resonance energy transfer experiments. *Biochemistry.* **40:** 5065–5074.